PVP—Vol. 98-8

Proceedings of the 1985
Pressure Vessels and Piping Conference

Fracture, Fatigue, and Advanced Mechanics

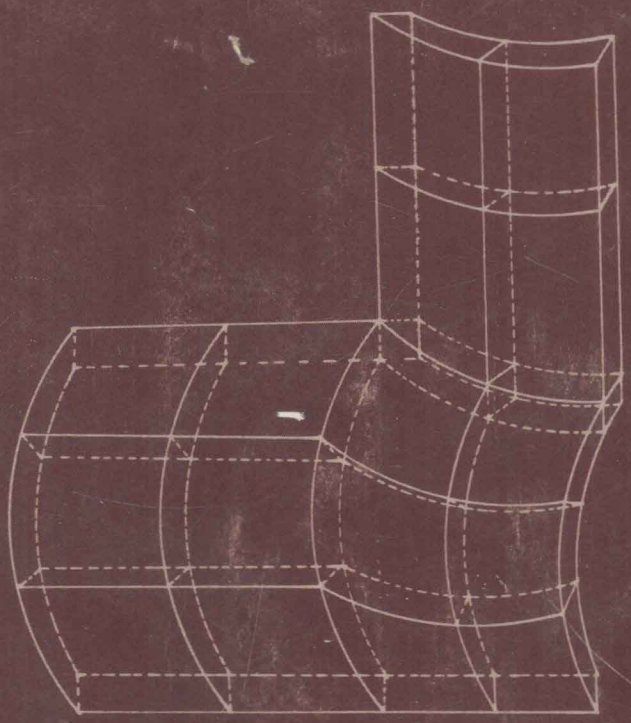

PVP—Vol. 98-8

Proceedings of the 1985
Pressure Vessels and Piping Conference

Fracture, Fatigue, and Advanced Mechanics

presented at

THE 1985 PRESSURE VESSELS AND PIPING
CONFERENCE AND EXHIBITION
NEW ORLEANS, LOUISIANA
JUNE 23–26, 1985

sponsored by

PRESSURE VESSELS AND PIPING DIVISION
DESIGN AND ANALYSIS COMMITTEE
HIGH PRESSURE TECHNOLOGY
SUB-COMMITTEE

Contributing Editors

G.E.O. WIDERA
R.J. MC GRATTAN
S.Y. ZAMRIK
S.K. BHANDARI
H.A. POHTO

Volume Coordinating Editors

W.E. SHORT
S.Y. ZAMRIK

General Proceedings Editor

S.J. BROWN

THE AMERICAN SOCIETY OF MECHANICAL ENGINEERS
United Engineering Center 345 East 47th Street New York, N.Y. 10017

PRESSURE VESSELS AND PIPING DIVISION
1985 PROCEEDINGS AND CONFERENCE

Technical Program Committee

Chairman	Sam Brown
Operations, Applications, and Components	G. Wilkowski G. Hollinger
Materials and Fabrication	D. Marriott
High Pressure Technology	H. Pohto
Design and Analysis	W.E. Short
Computer Technology	K.H. Hsu
Lifeline Earthquake Engineering	T. Ariman
Local Representatives	Fred Dumas Steve Mead

Volume 8 — Contributing Editors

G.E.O. Widera
University of Illinois
Chicago, Illinois

S.Y. Zamrik
Quest Engineering & Development Corp.
Crosby, Texas

R.J. McGrattan
General Dynamics Corp.
Groton, Connecticut

S.K. Bhandari
Novatome
Le Plessis-Robinson, France

H.A. Pohto
Martin Marietta Energy Systems Inc.
Oak Ridge, Tennessee

Volume 8 — Coordinating Editors

W.E. Short
ICI Americas Inc.
Wilmington, Delaware

S.Y. Zamrik
Pennsylvania State University
University Park, Pennsylvania

General Proceedings Editor

S.J. Brown
Quest Engineering & Development Corp.
Crosby, Texas

Library of Congress Catalog Card Number 85-71285

Proceedings of the 1985 Pressure Vessels and Piping Conference

Published in Nine Volumes

PVP—Volume 98-1
Residual-Life Assessment, Nondestructive Examination, and Nuclear Heat Exchanger Materials

PVP—Volume 98-2
Pressure Vessel Components Design and Analysis

PVP—Volume 98-3
Recent Advances in Seismic Design of Piping and Components

PVP—Volume 98-4
Seismic Performance of Pipelines and Storage Tanks

PVP—Volume 98-5
Computer-Aided Engineering

PVP—Volume 98-6
Structural Dynamics

PVP—Volume 98-7
Fluid-Structure Dynamics

PVP—Volume 98-8
Fracture, Fatigue, and Advanced Mechanics

PVP—Volume 98-9
Piping, Feedwater Heater Operation, and Pumps

FOREWORD

State-of-the-art engineering practices in pressure vessel and piping technology are the result of continual efforts in the evaluation of problems which have been experienced and the development of appropriate design and analysis methods for those applications. The resulting advances in technology benefit industry with properly engineered, safe, cost-effective pressure vessels and piping systems. To this end, advanced study continues in specialized areas of mechanical engineering such as fracture mechanics, experimental stress analysis, high pressure applications and related material considerations, as well as advanced techniques for evaluation of commonly encountered design problems.

This volume is comprised of current technical papers on various aspects of fracture, fatigue and advanced mechanics as related to the design and analysis of pressure vessels and piping.

The papers in this volume were prepared for presentation in technical sessions developed for the 1985 ASME Pressure Vessel and Piping Division Conference in New Orleans, La. The sessions on Design and Analysis of Pressure Vessels, Fracture and Fatigue of Pressure Vessels and Piping, and Thermal Fatigue and Thermal Striping were developed under the auspice of the Design and Analysis Committee. The sessions on High Pressure Technology are under the auspice of the Sub-Committee on High Pressure Technology.

While most of the individual papers in this volume were prepared for problems associated with a specific industry, much of these works can be applicable to other industries as well. Hence, the subject matter of the various papers may be suitable in analogous situations for the chemical, petro-chemical and nuclear industries.

W. E. Short

CONTENTS

DESIGN AND ANALYSIS OF PRESSURE VESSELS – I

G. E. O. Widera

All the papers in this session deal with some aspect of the design and analysis of pressure vessels, whether they be used for power generation, space and ocean exploration, coal gasification or other applications.

In the paper by Natarajan and Widera, a three-dimensional FEM analysis of a T-branch pipe connection under internal pressure loading is presented. Comparison with experimental results shows that the stress distributions and intensity factors can be predicted quite accurately. It is also shown that the normal stress index increases as d/D increases.

The paper by Batra and Sun presents the values of the rotational spring constants at the juncture of a radial nozzle and a spherical shell. It is shown that the value of this spring constant may be reduced by increasing the shell diameter and decreasing the shell thickness, nozzle diameter and nozzle thickness.

In his paper, Chao presents analytical solutions for stresses and displacements in spherical shells due to various types of loading over a rectangular area.

McGrattan employs energy methods to derive the equations needed to rapidly assess the minimum weight of cylindrical panels. Optimization techniques are applied to stress, stability and deflection constraints.

The paper by Pourmohamadian and Sabbaghian deals with the application of thermoelastoplastic theory using temperature dependent properties to determine the transient and residual stresses in a cooling solid cylinder.

THREE-DIMENSIONAL ANALYSIS OF A T-BRANCH PIPING CONNECTION

R. Natarajan and G. E. O. Widera
Mechanical Engineering Department
University of Illinois at Chicago
Chicago, Illinois

ABSTRACT

Regulatory authorities require one to prove that the main primary piping systems of nuclear power plants are safety protected against different types of damages. In particular, this proof has to be shown for normal and lateral branch connections. Failures of these connections are directly related to the peak stress resulting from different loadings. Thus, an in-depth parametric analysis of T-branch connections is necessary.

Experimental or numerical studies on intersections with diameter ratio larger than 0.5 are generally lacking. The present authors have therefore focused the attention on the diameter ratios of greater than 0.5. A brief description of the finite element model for T-branch connection is presented. Using this, four different diameter ratios have been studied. The results have been compared and the cost effectiveness is brought out.

NOMENCLATURE

D	= outside diameter of the main shell
d	= outside diameter of the nozzle
I_n	= stress intensity factor = σ/σ_n
P	= internal pressure
T	= thickness of the main shell
t	= thickness of the nozzle
σ	= maximum stress in the shell
σ_n	= hoop stresses in the shell
θ	= angle measured along nozzle-cylinder intersections

INTRODUCTION

The wide use of normally intersecting cylindrical shells in nuclear and fossil power plants, as well as petro-chemical industries, makes it an important, necessary and interesting topic for study. Further, regulatory authorities require one to prove that the main primary piping systems of nuclear power plants are safety protected against different types of damages. Among these are excessive deformation, elastic, plastic and elasto-plastic instability, fatigue, etc. In particular, this proof has to be shown for normal and lateral branch connections. Failures of these connections are directly related to the peak stress resulting from different loadings. Thus, an in-depth parametric analysis of T-branch connections is necessary.

Most of the analyses so far published have been limited to configurations where the ratio of the diameters of the branch to the main shell was less than 0.5 and for the range of the diameter to thickness ratio of the main shell from ten to hundred. Experimental or numerical studies on intersections with diameter ratio larger than 0.5 are generally lacking. The present authors have therefore embarked on a comprehensive research project with a focus on the diameter ratios of greater than 0.5. Further, the cost effectiveness of this study has to be examined if the analysis is to be extended to the in-elastic region.

In the following, a brief description of the finite element model for the T-branch connection is presented. Using this, four different diameter ratios have been studied. The results have been compared and the cost effectiveness is brought out.

IMPORTANCE OF THE PROBLEM

Of the different modes of failures to be guarded against in the design of high temperature and pressure bounded piping and components, fatigue failure due to peak stress resulting from cyclic loading is very complex to predict and very detrimental to the safety and reliability of power plants. Peak stress is the highest stress that a component or piping is subjected to in the presence of local geometrical discontinuites. The accurate determination of peak stresses in complex asymmetric and quasisymmetric configurations is neither practical nor feasible in all cases. For this reason, the design codes, such as the ASME Boiler and Pressure Vessel Code, Section III, and Division 2 of Section VIII [15], provide stress indices or concentration factors that can be readily used in design.

Section III of the ASME Code provides stress indices for nozzles in spherical shells, formed heads and cylindrical shells under low internal pressure loading only. The stress index method simply consists of

expressing the peak stress as a product of a multiplier called stress index and a known reference stress component such as the nominal hoop stress of a main pipe. The present code rules provide values of stress indices for pressure loading normal stress index estimate for $d/D < 0.15$.

Since the early analytical investigation of Bijlaard (1), there have been numerous other studies on this subject using both analytical and experimental methods. Raju (2,3,4) studied 45 degree lateral connections subjected to inplane moment and pressure loading using three-dimensional finite elements. The analyses were restricted to d/D ratios of 0.08 and 0.5. The shells considered were shallow since the value of $\lambda \left(= \frac{d}{Dt} \right.$, a measure of the inclusion size) was below 3.0. In the Conclusion section, suggestions were made for the study of lateral connections with $d/D > 0.5$ along with other loading conditions. In Reference 5, Steele studied the case of a radial nozzle loaded due to normal load and longitudinal and circumferential moment. He used Flügge-Conrad and Sanders-Simmonds solutions and developed a computer code named 'FAST'. It is worth mentioning that the case studies carried out, had $d/D < 0.5$. Here again, it was recommended that a more detailed analysis was necessary to study the effect of reinforcements on the stress indices. The above referred method of analysis was extended by Ranjan (6) to include three more loading cases. The computer code developed, called NUTSHELL, was capable of analyzing shell intersections with $d/D = 0.2$. Berger (7) discussed the stress distribution at the intersections, due to four moment loads, pressure load and thermal load, with the help of the finite element analysis. In that report, a case of d/D ratio greater than 0.5 was considered. Khan (8) compared the stress distribution in reinforced and unreinforced radial branchings of pipes under inplane, out of plane and internal pressure loading using the finite element method. With the help of a combination of eight noded brick and shell elements he showed excellent agreement of the stresses near the junction with experimental results. A similar type of finite element approach was used by Kozluk (9) for the analysis of a T-junction used in the Bruce Nuclear generating station 'A' steam generator. In this case sixteen unit loading conditions were taken into account (12 mechanical + pressure + 3 thermal loadings) but only one quarter of the geometry of the pipe assembly was considered. This was made possible by adjusting the boundary conditions. Zhixiang (10) studied both experimentally and numerically equal diameter tees and reported a good correlation between the results. The reinforced small opening vessel data presented as SHELLTECH report 81-5 has been recently published in the form of a WRC Bulletin (11) by Mershon et al. This bulletin presents the plots of stress resultants on the vessel for radial as well as two moment loads at the nozzle end. The ratio d/D is again limited to 0.5. Steele (12) extended his previous study on small openings in vessels, to large openings but the analysis is again restricted to rigid nozzles and due to external loads only. A wealth of experimental results for stress concentrations factors and flexibility factors are available in Ref. (13) but again they are restricted to $d/D < 0.5$.

From the above short review of progress made on the present topic, it is seen that studies have not been conducted on the effect of internal pressure pipe branch connections with $d/D > 0.5$, and, in particular, on lateral connections. The flexibility of the connection, an important aspect from the piping point of view, has also surprisingly been given very little attention so far. All the finite element analyses conducted have either used three-dimensional elements or shell elements. Furthermore, the analysis of the present problem is very expensive and a cost effectiveness study is very important when it is required to analyze the intersection problems for a large number of load cases and different geometries. This becomes even more critical when an in-elastic study needs to be conducted.

In the present paper a study of the T-branch pipe connection under internal pressure loading is attempted using 20-noded iso-parametric elements. A comparative study of the stress field in the intersection region of the two cylindrical shells with no reinforcement with other such published results are presented to show the validity of the present model as well as to examine the cost effectiveness.

FINITE ELEMENT ANALYSIS

The finite element analysis has been performed using a computer source code developed by the first named author [14]. The generation of the mesh and nodal coordinates are also incorporated in the program. In the analyses, 20-noded iso-parametric elements have been used and its stiffness generated with economical use of the elasticity matrix. The finite element representative distribution is shown in Fig. 1. Due to the symmetry of the structure and loading, only a quarter of the model was used for the analysis. The analysis was performed with two different mesh distributions to study the convergence with respect to the element size. By comparison, a model with 100 elements was found to be adequate. The complete model has everywhere one element though the thickness and has 818 nodes. The boundary conditions used in the analyses are as follows:

(a) Symmetry boundary conditions are imposed on symmetry surfaces.
(b) The free end of the branch pipe and the main shell are subjected to a longitudinal stress as obtained from the corresponding relation Pd/2t.

The finite element analyses have been carried out for four different ratios of d/D and the nominal dimensions of T-branch are shown:

	d_{inch}	D_{inch}	t_{inch}	T_{inch}	d/D
Model 1 (Ref. 8)	4.5	6.25	0.237	0.28	0.68
Model 2	4.5	9.0	0.237	0.28	0.5
Model 3	4.5	7.5	0.237	0.28	0.6
Model 4	4.5	6.0	0.237	0.28	0.75

RESULTS AND DISCUSSION

To check the validity of the present model, the elastic stress analysis of the T-branch with pipe dimensions as per Ref. 8 (Model 1) was used since, to the knowledge of the authors, it is the only analysis available for $d/D > 0.5$. The hoop and longitudinal stress on the main cylinder have been plotted and compared as shown in Fig. 2. The stress components are normalized by dividing them by "hoop stress" in the main shell. It has been seen that the hoop and longitudinal stress distribution obtained from the present finite element analysis agrees very well with those of Reference 8, thus validating the model for its accuracy. It is now thus possible to use the present three-dimensional finite element program for the parametric study of T-branch pipe connections.

It is a normal practice, in cylindrical pressure vessels, to assume that the effect of singularities are not felt after a distance of one diameter along the length of the cylinder. Thus to understand the importance of the end conditions of the shell, an analysis

was conducted with both the main shell end and branch shell end free. The length of the main shell was taken more than two times its diameter. The normalized hoop stress distribution is shown in Fig. 3 indicating the remarkable difference in the stress distribution. The comparison of the curves show that the bending produced on the main shell due to the presence of the nozzle is more prominent if the ends of the cylinder are considered free.

Having established a three-dimensional finite element model, a parametric study of the T-branch connection has been carried out. The contour plot of the normalized hoop stress at $\Theta = 180°$ has been calculated by interpolating the stresses obtained at the integration point in the element. Thus the stress index (as defined by ASME code NB-3683.1 (d)) has been calculated for the four models analyzed and is given as follows:

	σ_n	σ	I_n
Model 1	26.0	11.58	2.25
Model 2	29.5	15.6	1.89
Model 3	25.0	12.9	1.94
Model 4	24.0	10.20	2.35

CONCLUSIONS

(1) An effective three-dimensional finite element model has been developed for the analysis of T-branch pipe connections since the resulting stress distribution agrees very well with those already available in the literature.

(2) The number of elements used in the present study, conducted for comparison sake, is 100 and is much less than the corresponding member used in Reference 8. The stress distributions and stress intensity factors have been predicted quite accurately with the present model. The effect of end conditions on the stress distribution has also been studied accurately. Thus with lesser pre- and post-processing time as well as lesser execution time, it is now possible with the present model to study the T-branch connection accurately.

(3) Results for the normal stress index for four different d/D ratio have been reported and found to increase as d/D increases.

REFERENCES

1. Bijlaard, P.P., "Stresses from Local Loadings in Cylindrical Pressure Vessels," Trans. ASME, Vol. 77, 1955, pp. 805-816.
2. Raju, P.P., "Development of Stress Indices for 45 Lateral Connections via 3-D Finite Element Analysis," Proc. of 6th SMIRT, Paris, 1981, Paper No. F 3/4.
3. Raju, P.P., "A Parameter 3-D Analysis of 45 Degree Lateral Connections for the Development of Stress Indices," Proc. of 7th SMIRT, Chicago, 1984,
4. Raju, P.P., "3-D Analysis of a 45 Degree Lateral Connection with d/D = 0.5, D/T = 40 Under Internal Pressure and In-Plane Moment Loadings," ASME Paper No. 82-PVP-7.
5. Steele, C.R. and Steele, M.L., "Stress Analysis of Nozzles in Cylindrical Vessels with External Load," ASME Paper No. 82-PVP-14.
6. Ranjan, G.V., Brooks, G.N. and Huet, R., "An Improved Method of Stress Analysis for Cylinder-to-Cylinder Intersections," ASME Paper No. 82-PVP 41.
7. Berger, B.R., et al., "Finite Element Determination of Stress Indices," ASME Paper No. 82-PVP-12.
8. Khan, A.S., et al., "A Comparative Study of the Stress Field Around a Reinforced Normally Intersection Cylindrical Shell," ASME Paper No. 82-PVP-9.
9. Kozluk, M.J., et al., "Comparison of Finite Element Analysis of a Steam Generator Tee-Junction Using Shell and Solid Elements," ASME Paper No. 83-WA/PVP-4.
10. Jiang, Zhixiang, et al., "Stress and Strength Analysis of Equal Diameter Tees," Proc. of th International Conference on Pressure Vessel Technology, Vol. 1, Sept. 1984, pp. 220-235.
11. Mershon, J.L., Mokhtarian, K., Ranjan, G.V. and Rodabaugh, E.C., "Local Stresses in Cylindrical Shells due to External Loadings on Nozzles," Supplement to WRC Bulletin 107.
12. Steele, C.R., "Reinforced Openings in Large Steel Pressure Vessels: Solution for Large Openings," SHELLTECH Report 84-1, January, 1984.
13. Hayes, J.K., Moore, S.E., "Experimental Stress Analysis for Four 24-in. ANSI Standard B16.9 Tees," Jl. of Pressure Vessel Technology, No. 1977, pp. 537-552.
14. Thareja, D.V. and Natarajan, R., "Analysis and Design of Right Bifucating Pressure Tunnels," Int. Water Power and Dam Construction, Vol. 30, No. 9, No. 9, Sept. 1978, pp. 43-49.
15. Section IV, Division 1, ASME Boiler and Pressure Vessel Code, 1980 edition, American Society of Mechanical Engineers, New York, New York, 1981.

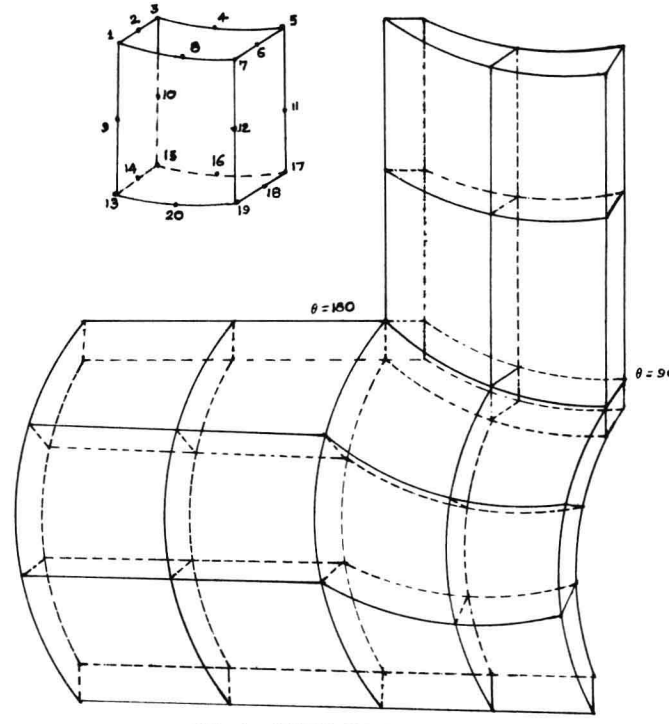

FIG. 1 FINITE ELEMENT MESH

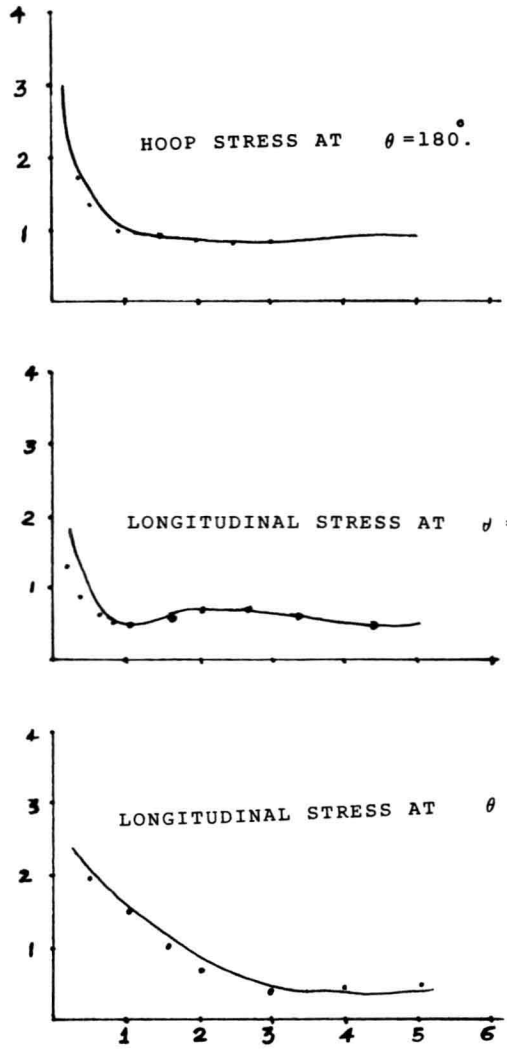

FIG. 2 STRESS DISTRIBUTION

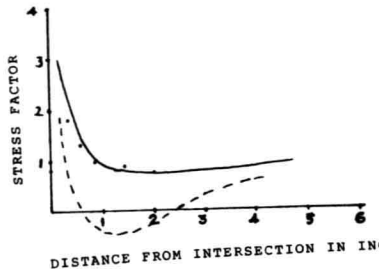

HOOP STRESS AT $\theta = 180^{\circ}$.

— REFERENCE 8.

• PRESENT ANALYSIS WITH END FORCES PRESCRIBED

--PRESENT ANALYSIS WITH ENDS FREE

FIG. 3 STRESS DISTRIBUTION

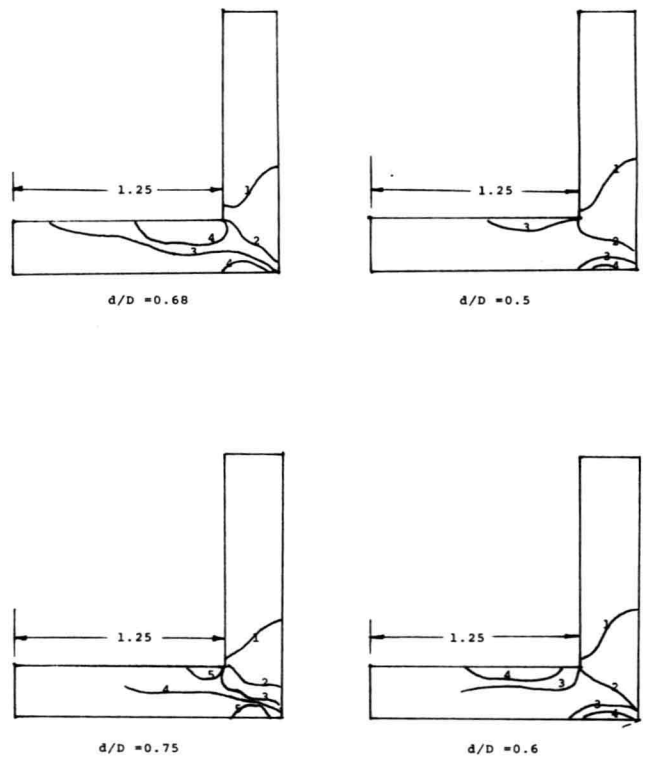

FIG. 4 STRESS CONTOURS

1→0.0
2→0.85
3→1.12
4→1.20
5→1.40

ON ROTATIONAL SPRING CONSTANTS AT THE JUNCTURE OF A RADIAL NOZZLE AND A SPHERICAL SHELL

B. Batra* and B. C. Sun, Associate Professor
Mechanical Engineering, New Jersey Institute of Technology
Newark, New Jersey

ABSTRACT

This paper presents the values of the rotational spring constants (i.e. Spring Constants due to bending moment) at the juncture of a radial nozzle and a spherical shell. This rotational spring constant is a function of diameters and thicknesses of nozzle and vessel. It is known that a lower Rotational Spring Constant at the juncture would reduce the local peak stresses which is very important in fatigue design of pressure vessel. This study shows that the value of the Rotational Spring Constant may be reduced by increasing the shell diameter and decreasing the shell thickness, nozzle diameter and nozzle thickness. Analytical derivations for this spring constant are presented in this paper. The actual values of Rotational Spring Constants for various nozzle-shell combination have been computed using a digital computer. These values are tabulated and plotted in this paper to facilitate the vessel design and stress analysis.

NOMENCLATURE

a = Radius of the middle surface of the radial nozzle

$A_{1,1}$ to $A_{4,4}$ = Constants

B_1 to B_4 = Constants

C_3, C_4, C_{12} = Constants

$D = Et^3/[12(1-\mu^2)]$ = Flexural Ridigity of spherical shell

D_1 to D_{12} = Constants

E_c = Modulus of elasticity at room temperature

E_h = Modulus of elasticity at temperature of operation

F = Stress Function

h = Thickness of the radial nozzle

H_1 to H_8 = Constants

K = Rotational Spring Constant

K_1 to K_5 = Constants

Ker s, Kei s, Ker u, Kei u = Kelvin functions of zero order

Ker's, Kei's, Ker'u, Kei'u = Derivatives of Kelvin functions

$l = [R^2t^2/(12(1-\mu^2))]^{1/4}$

L_1 to L_4 = Constants

M = Bending moment coming through a nozzle

M_o = Bending moment (M_x) in the nozzle at x=0

M_x = Radial moment acting per unit width upon a normal section of the spherical shell

M_y = Tangential moment acting per unit width upon a meridional section of the spherical shell

M_{xy} = Twisting moment in the nozzle or spherical shell

$N = Eh^3/[12(1-\mu^2)$ Flexural rigidity of nozzle

N_x = Radial membrane force, acting per unit width upon a normal section of the spherical shell

N_y = Tangential membrane force, acting per unit width upon a meridional section of the spherical shell

Q_x = Transverse shear force in cross-section of the nozzle

$\bar{Q}_x$ = Equivalent transverse shear force for nozzle in section upon which Q_x acts

Q_{xv} = Transverse shear force in cross-section of the spherical shell

$\bar{Q}_{xv}$ = Equivalent transverse shear force for spherical shell in section upon which Q_{xv} acts

*Currently Senior Product Design Engineer at General Electric Environmental Services, Inc., Lebanon, Pennsylvania

R = Radius of middle plane of spherical shell

r = Radius of curvature of middle surface of Spherical Shell in a latitudinal plane (Refer Fig. 1)

s = $r/l=1.81784(r/R).(R/t)^{\frac{1}{2}}$

t = Thickness of the spherical shell

T = Temperature of operation

T_x = Axial membrane force in the nozzle

T_y = Tangential membrane force in the nozzle

$T_{x\theta}$ = Membrane shear force in the nozzle

u = $a/l=1.81784(a/R).(R/t)^{\frac{1}{2}}$

u_1 = Axial displacement of the nozzle

v_1 = Displacement of the nozzle in the tangential (θ) direction

v_o = Transverse shear v_x in nozzle at x=0

w_1 = Radial deflection of the nozzle, positive if directed outwards

w_v = Radial deflection of the spherical shell, positive if directed outwards

x = Axial coordinate of cylindrical shell (nozzle)

y = Tangential coordinate of cylindrical and spherical shells

z = Radial coordinate of cylindrical shell (nozzle)

Greek Symbols

α = Slope angle at the juncture of spherical shell and nozzle with respect to their original positions due to their deflections

α_1 = $(1/a)[1-(1/2\mu)+(3(1-\mu^2)r^2+1-(3/4\mu^2))^{\frac{1}{2}}]^{\frac{1}{2}}$

β = R/t (A Shell Parameter)

β_o = $[3(1-\mu^2)/(a^2h^2)]^{\frac{1}{4}}$

β_1 = $(1/a)[-1+(1/2\mu)+(3(1-\mu^2)r^2+1-(3/4\mu^2))^{\frac{1}{2}})^{\frac{1}{2}}$

γ = a/h (A Nozzle Parameter)

ε = Unit strain

θ = Polar coordinate for spherical shell and nozzle, in radians

μ = Poisson's Ratio (Assumed as 0.3 for calculations)

ρ = t/h (Shell Thickness/Nozzle Thickness)

ϕ = Angle between shell axis and normal to middle surface of spherical shell, in radians

∇^2 = $(d^2/dr^2)+(1/r)(d/dr)$

INTRODUCTION

With the advent of more and more chemical plants, power plants and other process plants, the safety requirement and economy in design of pressure vessels are gaining high priority. This leads to the requirement of a more accurate stress analysis.

It is known that there exist highly localized stresses at the juncture of nozzle and pressure vessels, both in cylindrical and spherical tupes. However, these stresses cannot be accurately evaluated even with most modern and highly sophisticated computer programs without reliable values of the spring constants at these junctures. The radial spring constants at the juncture of a radial nozzle and a spherical shell are given in Ref [1]. This paper deals specifically with rotational spring constants (i.e. spring constants due to bending moment) at the juncture of a nozzle and a spherical shell.

Bijlaard has studied the differential equations for a bending moment acting on a spherical shell. His solution leads to the deflection of the spherical shell only [2]. He did not specify the relationships of rotational spring constants in terms of shell parameters (diameter and thickness) and the nozzle parameters (diameter and thickness). This part is explicitly developed here. The solution involves Kelvin functions of zero and first order along with their derivatives. These are obtained by programming the mathematical equations given by Abromowitz and Stegun [3].

DERIVATION OF EXPRESSION FOR DEFLECTION OF SPHERICAL SHELL DUE TO BENDING MOMENT

The radial deflection and stress function for the case of bending moment acting on the nozzle is given by [4]:

$$w_v = (C_3 Ker's + C_4 Kei's)\cos\theta \quad (1)$$

$$F = [Et^2/(12(1-\mu^2))^{\frac{1}{2}}].(C_3 Kei's - C_4 Ker's + C_{12}s^{-1})\cos\theta \quad (2)$$

where w_v = Radial deflection of spherical shell (in the direction of exterior normal)

F = Stress function

θ = Polar co-ordinate for cylindrical and spherical shells, in radians

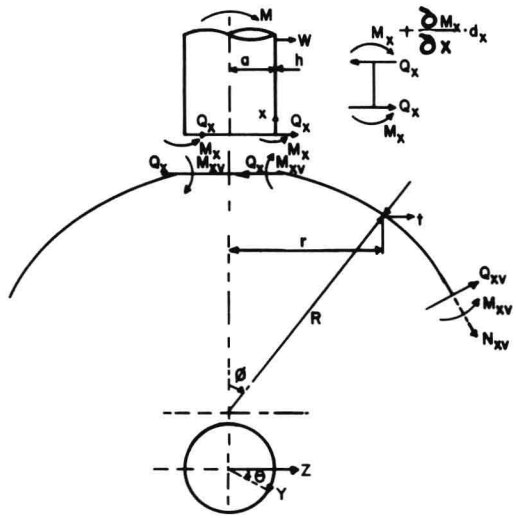

Fig.1 Spherical shell subjected to a bending moment (M) acting on a nozzle

The deflections of the nozzle in axial, tangential and radial directions are given by [2]:

$$u_1 = [e^{-\alpha_1 x}(H_5 \text{Cos } \beta_1 x + H_6 \text{Sin } \beta_1 x) - (M/(\pi ahE)).(x/a) - H_3 a].\text{Cos } \theta \quad (3)$$

$$v_1 = [e^{-\alpha_1 x}(H_7 \text{Cos } \beta_1 x + H_8 \text{Sin } \beta_1 x) - (M/(2\pi ahE)).(x^2/a^2) - H_3 x - H_4\ ] \quad (4)$$

$$w_1 = [e^{-\alpha_1 x}(H_1 \text{Cos } \beta_1 x + H_2 \text{Sin } \beta_1 x) + (M/(2\pi ahE)).(x^2/a^2) + 2\mu) + H_3 x + H_4] \quad (5)$$

Equations (1) and (2) contain 3 unknown constants, namely C_3,C_4 and C_{12} while equations (3),(4) and (5) contain 4 unknown constants, namely H_1,H_2,H_3 and H_4. (The constants H_5,H_6,H_7 and H_8 can be expressed in terms of constants H_1 and H_2 as per equations (27) and (40) of Ref. [2]). These 7 unknown constants require 7 boundary conditions between the spherical shell and the nozzle. These are given as follows:

Boundary Condition I:

The cross-section of the nozzle remains circular and its radius does not change. Hence B.C. I is given by:

$$(w_1)_{x=0} = 0 \quad (6)$$

Boundary Condition II:

Since the plane cross-section remains the same, the B.C. II is given by:

$$(u_1)_{x=o} = 0 \quad (7)$$

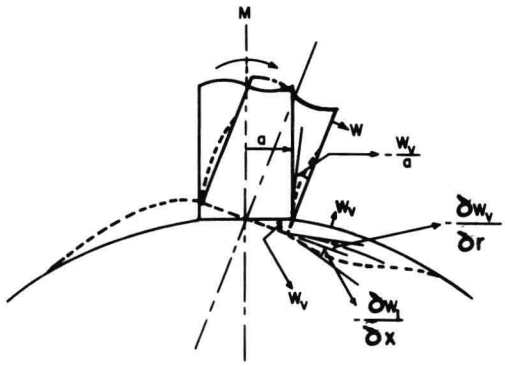

Fig.2 Deflections of nozzle and spherical shell due to a bending moment

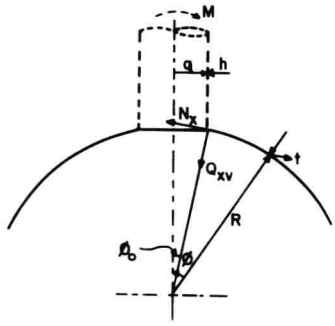

Fig.3 Normal and shear forces acting on the spherical shell at the nozzle-sphrical shell juncture

Boundary Condition III:

Since the shell is subjected to the external moment, we have from Ref. [5]:

$$C_{12} = [3(1-\mu^2)]^{\frac{1}{2}}.RM/(\pi Et^2 1) \quad (8)$$

Boundary Condition IV:

From Fig. 2, the compatibility of rotation at the juncture of spherical shell and nozzle requires:

$$-(\partial w_v/\partial r) - (\partial w_1/\partial x) = -w_v/a$$

$$\text{or, } (w_v/a - \partial w_v/\partial r)_{r=a} = (\partial w_1/\partial x)_{x=0} \quad (9)$$

Boundary Condition V:

The rotation of the spherical shell at r=a and that of nozzle at x=0 should be equal. This leads to:

$$(\varepsilon_{yv})_{r=a} = (\varepsilon_\theta)_{x=0} \quad (10)$$

Boundary Condition VI:

At the juncture, the bending moment M_x in the walls of the nozzle and shell should be equal. Hence, we set:

$$(M_{xv})_{r=a} = (M_x)_{x=0} \quad (11)$$

Boundary Condition VII:

The shear force Q_x in the nozzle at x=0 has to be in equilibrium with the horizontal components of the force in the shell at r=a. Hence from Fig. 1 and Fig. 3, we have:

$$N_x \text{Cos}\phi_o + \bar{Q}_{xv} \text{Sin}\phi_o = \bar{Q}_x$$

Here $\bar{Q}_{xv}$ and $\bar{Q}_x$ are the equivalent transverse shear forces for shell and nozzle respectively, including the effects of the twisting moments. Since ϕ_o is assumed to be small, this condition reduces to:

$$(1-a^2/2R^2)N_x + (a/R)\bar{Q}_{xv} = (Q_x)_{x=0} \quad (12)$$

Since boundary condition-III determine C_{12}, the rest six unknowns H_1,H_2,H_3,H_4, C_3 and C_4 are to be found using conditions I,II and IV through VII.

From conditions I & III, we set [2]:

$$H_4 = -H_1 - (\mu M/\pi ahE) \quad (13)$$

$$\text{and } H_3 = H_5/a \quad (14)$$

Using the remaining 4 conditions (i.e. IV through VII), the constants C_3,C_4, H_1 and H_2 can be found from equations (54),(59),(61) and (68) of Ref. [2]. These equations are numbered (15) to (18) in this paper and are given below:

$$D_1C_3 + D_2C_4 - [\alpha_1 - (L_1/a)]H_1 - [\beta_1 + (L_2/a)]H_2 = 0 \quad (15)$$

$$D_3C_3 + D_4C_4 - [(1+L_3)\gamma(12(1-\mu^2))^{\frac{1}{2}}/\rho u^2]H_1 - [L_4\gamma(12(1-\mu^2))^{\frac{1}{2}}/\rho u^2]H_2 = (1/\pi\mu)](\mu\rho^2/\gamma) - ((1+\mu).(12(1-\mu^2))^{\frac{1}{2}}/u^2)].(RM/Et^2 1) \quad (16)$$

$$D_5C_3 + D_6C_4 - D_7H_1 + D_8H_2 = [(2-\mu^2)/(12(1-\mu^2)\pi)].(RM/Et^2 1) \quad (17)$$

$$D_9C_3+D_{10}C_4+D_{11}H_1-D_{12}H_2=[(1-\eta)(12(1-\mu^2))^{1/2}/\pi u^3].(RM/Et^2 1) \quad (18)$$

where constants D_1 to D_{12} are given below:

$$D_1 = (u/a).[Kei\ u + (2/u)Ker'u] \quad (19)$$

$$D_2 = (u/a)[(2/u).Kei'u - Ker\ u] \quad (20)$$

$$D_3 = [(1+\mu)/u].Ker\ u + Ker'u + [2(1+\mu/u^2].Kei'u \quad (21)$$

$$D_4 = -[(1+\mu)/u].Kei\ u + Kei'u - [2(1+\mu)u^2].Kei'u \quad (22)$$

$$D_5 = [\gamma^2 u/(12(1-\mu^2))^{1/2}].[(1-\mu)u^{-1}.Kei\ u + 2(1-\mu)u^{-2}.Ker'u - Kei'u] \quad (23)$$

$$D_6 = [\gamma^2 u/(12(1-\mu^2))^{1/2}].[-(1-\mu)u^{-1}.Ker\ u + 2(1-\mu)u^{-2}.Kei'u + Ker'u] \quad (24)$$

$$D_7 = [\gamma^2 a^2/\rho^3 u(12(1-\mu^2))^{1/2}].[\alpha_1^2-\beta_1^2-\mu(1+L_3)/a^2 + (\alpha_1 L_1+\beta_1 L_2)/a] \quad (25)$$

$$D_8 = [\gamma^2 a^2/(\rho^3 u(12(1-\mu^2))^{1/2}].[2\alpha_1\beta_1 + \mu L_4/a^2-(\alpha_1 L_2-\beta_1 L_1)/a] \quad (26)$$

$$D_9 = (1-\eta)u^{-1}(Ker\ u-2u^{-1}Kei'u) - [u^3\rho^2/(12(1-\mu^2)\gamma^2)].[(1-\mu)u^{-2}\ Kei\ u - Ker\ u+u^{-1}.Kei'u + 2(1-\mu).u^{-3}.Ker'u\ ] \quad (27)$$

$$D_{10} = (1-\eta).u^{-1}.(Kei\ u+2u^{-1}.Ker'u) + [u^3\rho^2/(12(1-\mu^2))\gamma^2].[(1-\mu)u^{-2}.\ Ker\ u + Kei\ u+u^{-1}Ker'u-2(1-\mu).u^{-3}.Kei'u] \quad (28)$$

$$D_{11} = [a^3/(u^2\rho^2\gamma(12(1-\mu^2))^{1/2}].[\alpha_1(\alpha_1^2-3\beta_1^2) - (2-\mu)\alpha_1/a^2+(3-\mu)(-\alpha_1 L_3-\beta_1 L_4)/(2a^2) + (\alpha_1^2-\beta_1^2)L_1+2\alpha_1\beta_1 L_2)/a+(1-\mu)L_1/(2a^3)] \quad (29)$$

$$D_{12} = [a^3/u^2\rho^2\gamma(12(1-\mu^2))^{1/2}].[\beta_1(3\alpha^2-\beta_1^2) - (2-\mu)\beta_1/a^2-(3-\mu)(-\alpha_1 L_4+\beta_1 L_3)/(2a^2) - ((\alpha_1^2-\beta_1^2)L_2-2\alpha_1\beta_1 L_1)/a-(1-\mu)L_2/(2a^3)] \quad (30)$$

where α_1 and β_1 are given by Eq. (11) of Ref. [2] and are as follows:

$$\alpha_1 = (1/a).[1-1/(2\mu)+(3(1-\mu^2)\gamma^2+1-3/(4\mu^2))^{1/2}]^{1/2} \quad (31)$$

$$\beta_1 = (1/a).[-(1-(1/2\mu)+(3(1-\mu^2)\gamma^2+1-3/(4\mu^2))^{1/2}]^{1/2} \quad (32)$$

The constants L_1 to L_4 are as follows:

$$L_1 = K_1/K_5 \quad (33)$$

$$L_2 = K_2/K_5 \quad (34)$$

$$L_3 = K_3/K_5 \quad (35)$$

$$L_4 = K_4/K_5 \quad (36)$$

where constants K_1 to K_5 are as given below:

$$K_1 = a\alpha_1[(1-\mu).(1-3\mu(1+\mu+\mu^2))-12(1-\mu^4)\gamma^2 + (2(1-\mu).(2+3\mu+3\mu^2)+24\mu(1-\mu^2)\gamma^2)a^2\beta_1^2] \quad (37)$$

$$K_2 = -a\beta_1[(1-\mu).(1-3\mu(1+\mu+\mu^2))-12(1-\mu^4)\gamma^2 - (2(1-\mu).(2+3\mu+3\mu^2)+24\mu(1-\mu^2)\gamma^2)a^2\alpha_1^2] \quad (38)$$

$$K_3 = (1-\mu)(3+\mu)(1-3\mu^2)+12(1-2\mu-\mu^2)(1-\mu^2)\gamma^2 \quad (39)$$

$$K_4 = 2[(4+9\mu+3\mu^2)(1-\mu)+12(2+\mu)(1-\mu^2)\gamma^2]a^2\alpha_1\beta_1 \quad (40)$$

$$K_5 = [12(1-\mu^2)\gamma^2+(1-\mu).(1+3\mu)]^2 \quad (41)$$

Thus the final solution for the deflection of the spherical shell due to a bending moment M is given by equation (1) where constants C_3 and C_4 are obtained by solution of 4 simultaneous equations (15) to (18) for 4 unknowns; namely C_3,C_4,H_1 and H_2. The other constants; namely D_1 to D_{12}, L_1 to L_4, K_1 to K_5, α_1 and β_1 used in these equations are given by equations (19) to (41).

APPROACH FOR EVALUATION OF ROTATIONAL SPRING CONSTANTS

The expression for deflection

$$w_v = (C_3Ker's + C_4Kei's)Cos\ \theta \quad (1)$$

is valid at any point of spherical pressure vessel specified by radius r. Since, we are interested only in the deflection of the vessel at the juncture of nozzle and spherical shell, we let r=a.

At r=a, s=a/l=u

Also, for present analysis θ=0 since we are interested in maximum deflection due to moment which occurs in the plane where the moment is acting. Hence, the expression for w_v for this case becomes:

$$w_v = C_3Ker'u + C_4Kei'u \quad (42)$$

where $u = a/l = a.[12(1-\mu^2)/R^2t^2]^{1/4}$

Substituting μ=0.3, we set:

$$u = 1.81784.a/\sqrt{Rt} \quad \text{or}$$

$$u = 1.81784.(a/R)\sqrt{R/t} \quad (43)$$

The rotational spring constant due to bending moment is given by referring to Fig. 4:

$$K_B = M/|\phi| \quad (44)$$

From Fig. 4:

$$w_v = \phi.a$$

$$|\phi| = |w_v|/a$$

Substituting this expression for ϕ in equation (44), we set:

$$K_B = M.a/|w_v| \quad (45)$$